Electronic Supplementary Material (ESI) for RSC Advances.

Supplementary Information

Title: Rapid deterioration in buried leather: Archaeological implications

Authorship: Halldórsdóttir, H.H., Williams, R., Greene, E.M., Taylor, G.

Table 1.0: Bond vibrations and FTIR peaks commonly seen in the spectra of skin, vegetable tannins and oils. Full citations provided separately at the end of this document.

Component	Peaks (cm^{-1})	Indication	Citation
Collagen	↑ Amide I (1700-1600) & II (1580-1510)	Hydrolysis of collagen	(Albu et al., 2010)
	Δ Amide I & II position	collagen denaturation and gelatinisation	
	Amide III: 1400-1200	The 1450 cm^{-1} peak is associated with good collagen triple helix integrity	(Sendrea et al., 2016)
Vegetable tannin	1615-1601 | 1518-1507 & 1452-1446 | 1211-1196 & 1043-1030	Associated with all classes of tannins	(Falcão and Araújo, 2018)
	1288-1282, 1162-1155, 1116-1110, 872-870	Characteristic peaks for condensed tannins	
	1731-1704 with 1325-1317 region	Hydrolysable tannins – condensed tannin peaks	
	1088-1082, 872-870, or 763-758	Presence of gallotannin, identified by presence of weak bands	
Lipids	Symmetric & asymmetric CH_2 stretching at ~2920 and 2850	Attributed to lipids. Although, the ~1750 cm-1 peak has also been associated with peptide oxidation in FTIR analyses of	(Greve et al., 2008, Sommer et al., 2017,

	a C=O stretching at ~1750	historical parchment and leather.	Odlyha, 2007, Carsote and Badea, 2019, Derrick, 1991)
	CH_2 twisting at ~1300		
Other components	~1000	Silicates, common in FTIR spectra of soil	(Kögel-Knabner, 2002, Xu et al., 2019, Xu et al., 2020)
	Gypsum | 1110 Calcium stearate | 1575 & 1415 $CaCO_3$ | 875	Assigned to the use of metal soaps to remove excess fat from historical book leather.	(Vichi et al., 2018)
	2900, 1701, 1453 & 1383	Associated with the presence of underlying resins after analysis of historical gilt and painted leather by FTIR	(Vichi et al., 2018)
Collagen Ratios	Amide A/amide I ratio (AA/AI)	Associated with degree of crosslinking. Higher values indicate dissolution of crosslinking	(Albu et al., 2010, Vyskočilová et al., 2019, Sendrea et al., 2016)
	Amide I/amide II ratio (AI/AII)	Indicates hydrolysis of the collagen secondary structure chain	(Albu et al., 2010)
	Amide III/1450 cm-1 ratio (AIII/1450)	Assess triple helix conformity	

	Ratio of the two shoulders at ~1620 cm-1 and ~1650 cm-1 (1620/1650)	Assess extent of denaturation in waterlogged leather samples	(Godfrey and Kasi, 1998)
	Difference between wavenumber positions of the highest absorption in amide I and II peaks (ΔI/II)	Higher values associated with collagen denaturation and gelatinisation	(Albu et al., 2010, Vyskočilová et al., 2019)

Table 2.0 Leather and soil sample archaeological context description, including soil pH measurement results and notes on preservation, provided by the Vindolanda Trust.

Context	Soil pH	Time Period	date	Context Type	Colour	Composition	Texture	Inclusion	Preservations notes
V18-44	5.67-6.04	Antonine	213-275	Clay packing above wattle, daub and stone building	Dark greybrown	Clay	Firm	Large stones	Two leather shoes and scrap leather
V18-51	5.64-6.08	Antonine	180-200	Top fill of Antonine ditch	Greenish black grey	Silt, mud and laminate	Soft to Firm	Finds	High amounts of leather and wood, 64 leather items and scraps
V18-54	5.85-6.83	Antonine	213-275	Wattle and daub drain	dark brown	Silty Soil	Soft	Organics	One leather shoe and leather scraps
V18-57	6.15-6.25	Severan	200-212	Top fill of Several Ditch	Grey	Silty Clay	Soft to Firm	Organics	Seven leather items
V18-61	5.18 -5.51 pot, bone	Antonine	140-180	Bottom of Antonine ditch	Dark greenish brown	Mud	, Soft	Organics	Seven leather items

V18-62	4.96-6.08	Antonine	180-200	Antonine ditch fill	Dark green grey	Laminate and silt	Soft	Pot, bone	Six leather shoes and scrap leather
V18-71	5.64-5.74	Severan	200-212	Ditch mud	Dark greybrown	Mud and silt	Soft	Organics	Five leather items, leather scraps, wood and finds

Table 3.0: Parameters of the TQ analyst quantitation file used to collect peak absorbances from vegetable-tanned leather samples. Peak heights and baselines were given as ranges to account for possible shifts caused by bond variations.

	Peak Wavenumbers			Baseline Wavenumbers		
Peak ID	**Datapoint Type**	**Min Range (cm^{-1})**	**Max Range (cm^{-1})**	**Datapoint Type**	**Min Range (cm^{-1})**	**Max Range (cm^{-1})**
P3300	Max height in range	3111	3450	Max height in range	1770-1900	3600-3700
P3010	Max height in range	2900	3020	Max height in range	2750-2760	3000-3050
P2955	Max height in range	2950	2965	Max height in range	2750-2760	3000-3050
P2920	Max height in range	2900	2940	Max height in range	2750-2760	3000-3050
P2850	Max height in range	2835	2885	Max height in range	2700-2770	2975-3055
P1740	Max height in range	1730	1755	Max height in range	1690-1725	1760-1790
P1720	Max height in range	1680	1725	Max height in range	1670-1680	1725-1735
P1650	Max height in range	1640	1670	Max height in range	850-900	1780-1800
P1620	Max height in range	1590	1645	Max height in range	850-900	1780-1800
P1575	Max height in range	1560	1580	Max height in range	850-900	1780-1800
P1535	Max height in range	1520	1560	Max height in range	1470-1500	1550-1590
P1515	Max height in range	1495	1520	Max height in range	1470-1500	1550-1590
P1450	Max height in range	1435	1465	Max height in range	1385-1425	1475-1490
P1400	Max height in range	1380	1410	Max height in range	1250-1270	1405-1430
P1365	Max height in range	1365	1385	Max height in range	1250-1270	1405-1430
P1335	Max height in range	1325	1345	Max height in range	1250-1270	1405-1430
P1315	Max height in range	1295	1320	Max height in range	1250-1270	1405-1430
P1225	Max height in range	1210	1235	Max height in range	890-950	1250-1290
P1200	Max height in range	1190	1205	Max height in range	890-950	1250-1290
P1160	Max height in range	1035	1185	Max height in range	890-950	1250-1290
P1080	Max height in range	1065	1090	Max height in range	890-950	1250-1290
P1030	Max height in range	1010	1054	Max height in range	890-950	1250-1290

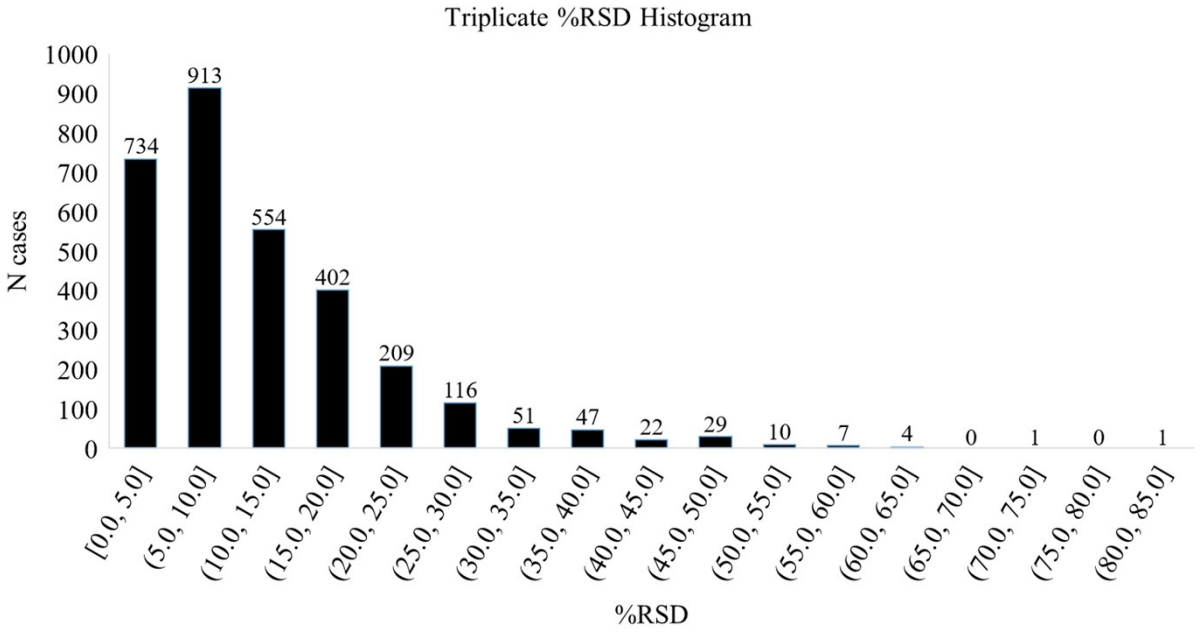

Figure 1.0: Relative standard deviations (%RSD) between triplicate measurements of modern experimentally buried leather samples

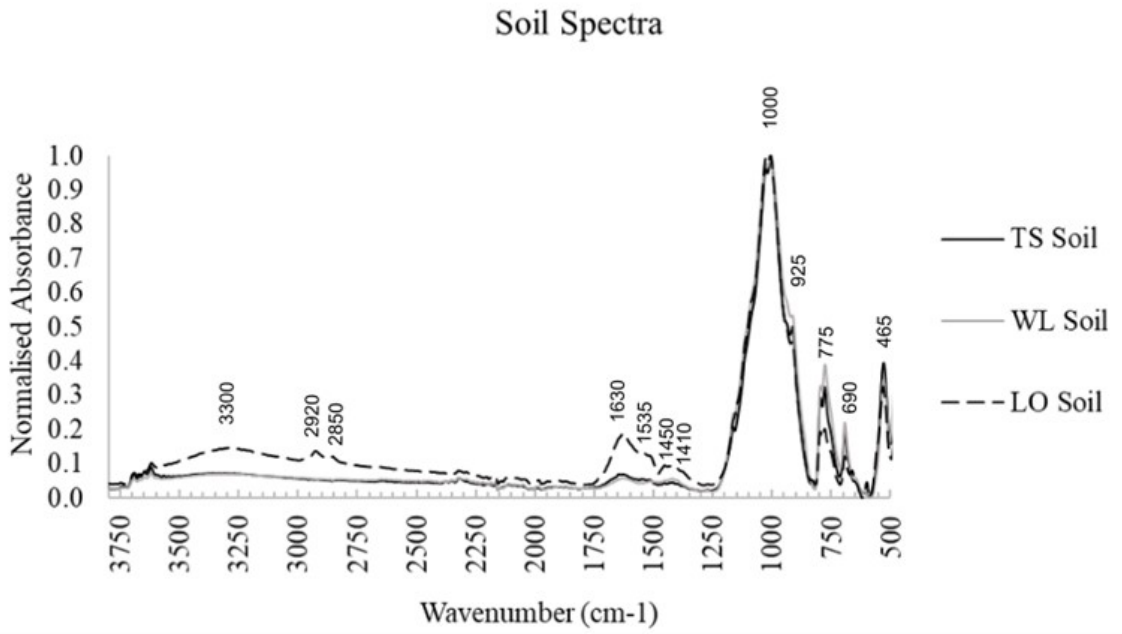

Figure 2.0: FTIR spectra of the microcosm soils. TS = typical soil, WL = waterlogged soil, LO = low oxygen soil

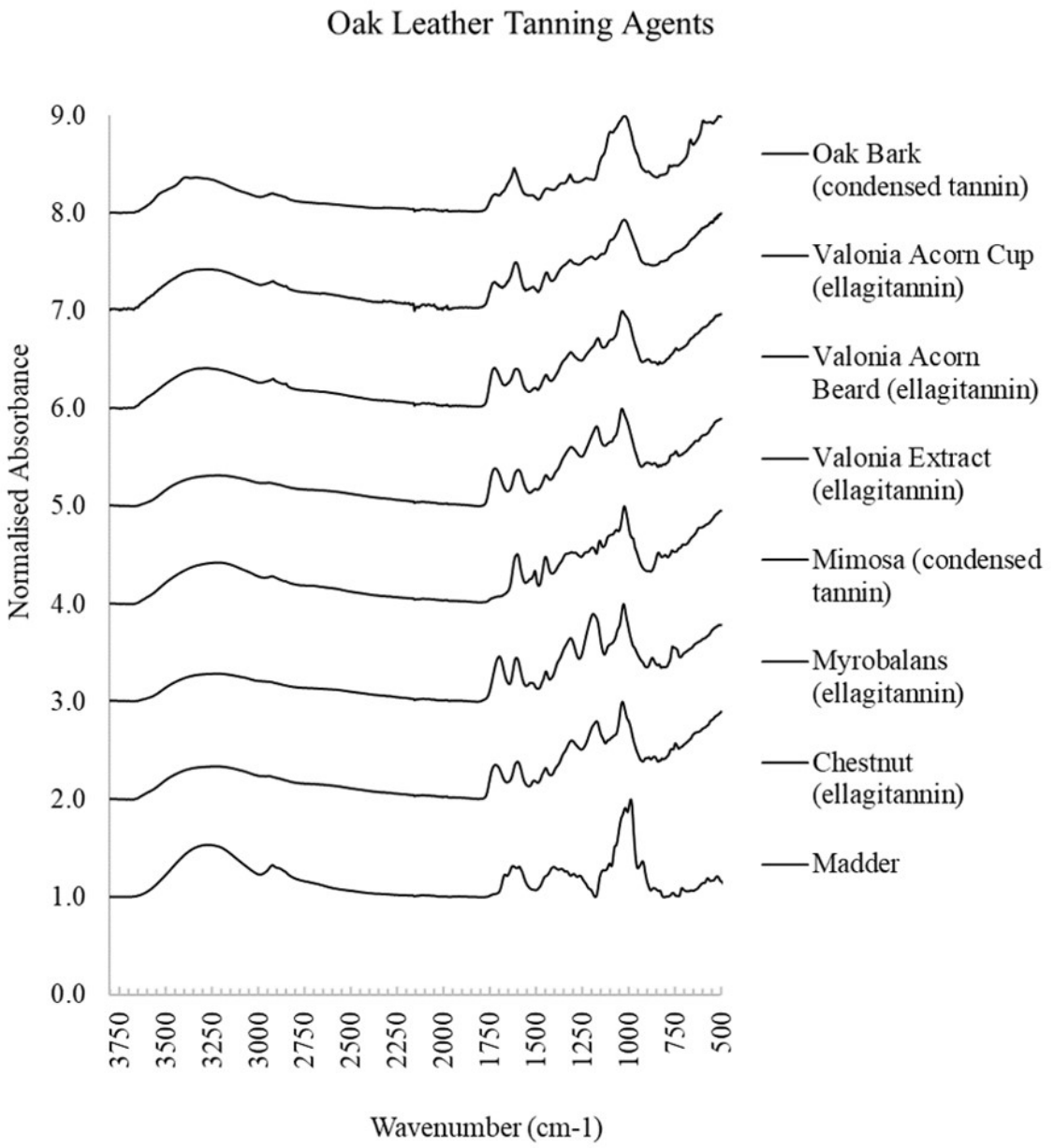

Figure 3.0: FTIR spectra of tanning agents for oak leather samples

Supplementary Information References

ALBU, M. G., GHICA, M. V., LECA, M., POPA, L., BORLESCU, C., CREMENESCU, E., GIURGINCA, M. & TRANDAFIR, V. 2010. Doxycycline delivery from collagen matrices crosslinked with tannic acid. *Molecular Crystals and Liquid Crystals,* 523**,** 97/[669]-105/[677].

CARSOTE, C. & BADEA, E. 2019. Micro differential scanning calorimetry and micro hot table method for quantifying deterioration of historical leather. *Heritage Science,* 7.

DERRICK, M. 1991. Evaluation of the state of degradation of Dead Sea Scroll samples using FT-IR spectroscopy',. *The Book and Paper Group Annual,* 10**,** 49-65.

FALCÃO, L. & ARAÚJO, M. E. M. 2018. Vegetable tannins used in the manufacture of historic leathers. *Molecules,* 23.

GODFREY, I. & KASI, K. 1998. The analysis and treatment of waterlogged leather I: Denaturation and defibrilisation studies.

GREVE, T. M., ANDERSEN, K. B. & NIELSEN, O. F. 2008. ATR-FTIR, FT-NIR and near-FT-Raman spectroscopic studies of molecular composition in human skin in vivo and pig ear skin in vitro. *Spectroscopy,* 22**,** 437-457.

KÖGEL-KNABNER, I. 2002. The macromolecular organic composition of Plant and microbial residues as inputs to soil organic matter. *Soil Biology and Biochemistry,* 34**,** 139-162.

ODLYHA, M. 2007. Thermoanalytical (macro- to nanoscale) techniques and non-invasive spectroscopicanalysis for damage assessment of parchment. *In:* LARSEN, C. S. (ed.) *IDAP: Improved Damage Assessment of Parchment. Assessment, data collection and sharing of knowledge. Research Report no 18.* Luxembourg:: European Communities.

SENDREA, C., CARSOTE, C., BADEA, E., ADAMS, A., NICULESCU, M. & IOVU, H. 2016. NON-INVASIVE CHARACTERISATION OF COLLAGENBASED MATERIALS BY NMR-MOUSE AND. *U.P.B. Scientific Bulletin, Series B,,* 78**,** 27-38.

SOMMER, D. V. P., MÜHLEN AXELSSON, K., COLLINS, M. J., FIDDYMENT, S., BREDAL-JØRGENSEN, J., SIMONSEN, K. P., LAURIDSEN, C. B. & LARSEN, R. 2017. Multiple Microanalyses of a Sample from the Vinland Map. *Archaeometry,* 59**,** 287-301.

VICHI, A., ELIAZYAN, G. & KAZARIAN, S. G. 2018. Study of the Degradation and Conservation of Historical Leather Book Covers with Macro Attenuated Total Reflection-Fourier Transform Infrared Spectroscopic Imaging. *ACS Omega,* 3**,** 7150-7157.

VYSKOČILOVÁ, G., EBERSBACH, M., KOPECKÁ, R., PROKEŠ, L. & PŘÍHODA, J. 2019. Model study of the leather degradation by oxidation and hydrolysis. *Heritage Science,* 7.

XU, X., DU, C., MA, F., SHEN, Y., WU, K., LIANG, D. & ZHOU, J. 2019. Detection of soil organic matter from laser-induced breakdown spectroscopy (LIBS) and mid-infrared spectroscopy (FTIR-ATR) coupled with multivariate techniques. *Geoderma,* 355.

XU, X., DU, C., MA, F., SHEN, Y. & ZHOU, J. 2020. Forensic soil analysis using laser-induced breakdown spectroscopy (LIBS) and Fourier transform infrared total attenuated reflectance spectroscopy (FTIR-ATR): Principles and case studies. *Forensic Science International,* 310.